Supporting Information

Self-regenerating 3D sponge evaporator with tunable porous structure for efficient solar desalination

Patsaya Anukunwithaya[a], J. Justin Koh[b], Jayven Chee Chuan Yeo[b], Siqi Liu[a], Xunan Hou[a], Nanxue Liu[ac] and Chaobin He*[, ab]

[a]Department of Materials Science and Engineering, National University of Singapore, 9 Engineering Drive 1, Singapore 117575, Singapore

[b]Institute of Materials Research and Engineering, Agency for Science, Technology and Research (A*STAR), 2 Fusionopolis Way, Innovis, Singapore 138634, Singapore

[c]Department of Materials Science and Engineering, Shanghai University, 99 Shangda Road, Baoshan District, Shanghai 20444, China

1. Materials and Chemicals

Low molecular weight chitosan (CS, Mw 50-190 kDa, 75 – 85% deacetylation), glycerol (molecular biology, ≥99.0%), glacial acetic acid (ACS reagent, ≥99.7%), and sodium dodecyl sulfate (SDS, ACS reagent, ≥99.0%), phosphate buffer saline (PBS, molecular biology, pH 7.2 – 7.6), ethanol (ACS reagent, ≥99.5%), methylene blue (Biological strain commission; ≥82.0%) and sodium chloride (NaCl, ACS reagent, ≥99.9%) were purchased from Sigma-Aldrich. Agarose (Aga, SeaKem®LE agarose, electrophoresis, gel strength >1,200 g/cm^2) was purchased from Lonza. Multi walled carbon nanotube (MW, -COOH 1.55% wt., >90.0%) was purchased from Cheaptubes. All chemicals were used without further purification. Milli-Q water (resistance ~18 MΩ) was used for all solution preparation throughout the experiment. Seawater was collected from West Coast beach and filtered with Ø 0.45 μm filter paper prior to the tests.

2. Method

2.1. *Preparation of the CS/Aga-MW sponge evaporator*

The preparation of the bio-based CS/Aga-MW sponge was totally prepared for 50 ml. First, 0.1 g of MW was dispersed in DI water using homogenizer. Then 1.67 g of CS and 0.1 g of SDS were added into 39.25 ml of MW solution. The black solution was stirred at room temperature for 15 min before adding 0.5 ml of acetic acid. The black slurry was stirred at room temperature for overnight to get fully dissolved CS-MW gel. After that, 4% wt. Aga was prepared at 90 ºC. Consequently, the clear Aga solution was added to the CS-MW at 80 ºC. The black gel was continue stirring at 80 ºC for 3 h. Glycerol (2 ml) was added to the reaction and stirred at 60 ºC for 1 h. The CS/Aga-MW gel was poured into cylindrical tube as the monolithic mold before freeze casting at -20 ºC for 24 h. The as-prepared hydrogel was immediately transferred for freeze drying process. Finally, the 5CS/Aga-MW sponge evaporator was obtained. The 1, 3 and 7CS/Aga-MW were prepared with the same process at the weight ratio of CS to Aga at 1:1, 3:1 and 7:1, respectively. Also, the CS- and Aga-MW sponges were fabricated as controlled samples. The resulting aerogels were then immersed into 0.1M PBS in 20% ethanol several times to remove all residue.

2.2. Characterizations

The macro/microstructure of the bio-based sponge evaporators were characterized via scanning electron microscope (SEM, ZEISS; Supra40) with an accelerating voltage of 5.0 kV. The dispersion of MW in polymer matrix was obtained using transmission electron microscope (TEM, JEOL; 2100F) with an accelerating voltage of 200 kV. The cyclic compression recovery performance was tested using Universal Testing Machine (UTS, Instron; 5900) with the compression rate was 150%/min under a cyclic profile of 100 compression test. The light

absorption was carried out by ultraviolet-visible-near infrared spectrometer (UV-vis-NIR, Agilent; Cary 5000). Absorption (%A) was calculated by %A = 1 – %T − %R. Differential Scanning Calorimetry (DCS, TA instruments; DSC25) was conducted for pure water and fully-swollen samples. The test was carried out in opened T-zero pans without lids, from 20 to 180^{o}C with a rate of 5^{o}C/min. The crystal was observed by x-ray diffractometer with Cu Kα radiation (XRD, Bruker; D8 advance). Polarized optical microscope (Nikon; Eclipse LV100ND) was used to obtain birefringent crystals. Fourier-transform infrared spectroscopy (ATR-FTIR, Agilent;Cary 660 spectrometer with Pike Gladi ATR) was measured in the wavenumber range of 500–4000 cm^{-1} range, with a resolution of 4 cm^{-1} and 64 scans. The surface temperature measurements and infrared images were taken by a thermal imaging camera (Seek, Shot Pro). Salinity of brine and purified water were determined by elemental analysis through an inductively coupled plasma-optical emission spectrometer (ICP-OES, Perkin Elmer Optima 5300DV).

3. Intermolecular hydrogen bond formation between CS and Aga

The FT-IR spectra in Fig. S1c. show broad bands signals of the 1, 3, 5, and 7CS/Aga-MW at 3200 - 3400 cm^{-1}, decreasing in their intensities and red shifting compared to neat CS and Aga. This indicates the intermolecular hydrogen bond between NH_2 and OH in the bio-based CS/Aga-MW composited aerogel. Also, the decreased amide II at 1,550 cm^{-1} peaks of all composited CS/Aga-MW in Fig. S1d. are presented relative to that of CS-MW. Furthermore, the characteristic peak at 1,375 cm^{-1}, attributed to amide III slightly shifted to a higher frequency, indicating that the molecular hydrogen bond was established between CS and Aga. Also, the intensified amide (III) signal can be observed due to the overlapped vibrational signal of the amide III in CS and isopropyl group attached to OH in Aga.[1-4]

4. Water diffusion/transport test

To study the water transport of the various samples, all composited sponge evaporators (with the dimension of 10 mm in height and 14 – 20 in diameter) were prepared. Then dry cellulose papers (15 mm in diameter) were put on top of each sample prior to their contact with water at the bottom. The time was recorded during the test.

To study vertical transport methylene blue for 1CS/Aga and 5CS/Aga sponges, the composited sponge (with the dimension of 30 mm in height and 20 ± 2 mm in diameter) were cut. Then the cutting composite sponges were put in the plastic petri dish before methylene blue solution was added into the specimens dish. The time was recorded during the test.

5. Water saturation content at equllibrium test

The water saturation content at equilibrium was determined by water absorbing experiment. All composited sponge were immersed into DI water for 48 hours. Then the filter paper was used to remove surface water at each weighing. The total mass of the absorbed water was obtained via measuring the mass change of the aerogel samples before and after water saturation. The saturated water per unit gram (SWG) was calculated according to Equation 1.

$$(M_w - M_d) / M_d \quad (1)$$

Where M_w and M_d are the weight of the fully swollen sponges and the corresponding dried sponges, respectively.

6. Solar Evaporation Experiments

DI Water, 3.5% wt. NaCl solution and seawater were used for the solar evaporation test. Evaporation tests were conducted using a solar simulator (Newport; 92250A-1000 with AM1.5G filter). The illumination intensity was calibrated to 1 kW m^{-2} or 1 sun, using thermopile (Newport; PVM914), connected with power meter (Newport; 91150). The mass change of water was

automatically recorded by an electronic balance (Sartorius; EntrisII with resolution of 0.001 g) at every 10 min. The area of the light exposed top area was 4.9×10^{-4} m^2 under 1 sun irradiation. All the evaporation experiments were performed at ~24 ^oC and relative humidity of ~70%.

7. Simulated salt regeneration test

The simulated salt regeneration test with 0.8 g of NaCl on top of the 5CS/Aga sponge evaporators in which 3.5% w/v. NaCl with temperature of 25ºC/humidity of 70%. The photographs were captured with time changed to observe salt crystals at the top of evaporators.

8. Calculation of light-to-heat energy conversion efficiency (η)

A water evaporation performance of the bio-based evaporators is also expressed in terms of light-to-heat conversions using the Equation 2.[5, 6]

$$\eta = [(\Delta m)(H_{lv} + Q)] / C_{opt}P_{in} \quad (2)$$

where Δm denoted the stable state of the water evaporation rate, subtracted by the water evaporation rate at dark conditions, H_{lv} is the enthalpy of water vaporization from the composite sponge evaporator which can be calculated from $H_{lv} = 1{,}918.46 \times (T(K)/T(K) - 33.91)^2$ $J \cdot g^{-1}$ [7, 8] (the H_{lv} was better calculated from the actual surface temperature as our bio-based composited sponges contain macropore structure, which brought up to bulk water forming at the evaporative surface), Q is the sensible heat of water at changing temperature (4.2 $J \cdot g^{-1}K^{-1}$), C_{opt} represents the optical concentration at the irradiated surface, P_{in} refers to the solar irradiation power of one sun (1 $kW \cdot m^{-2}$).

9. The overall energy transfer of solar evaporator followed by conservative rule

In the system, the solar radiation is only input energy for the water evaporation while energy loss from radiative heat loss between the composite sponge evaporator – water and air interface, the convective heat loss of the evaporator to an overlying air, and heat conduction loss of it to

underlying bulk water. From energy conservative rule, the evaporation energy due to the evaporator is related to the following parameters as shown in the Equation 3 and 4.[9-11]

$$E_{eva} = [(\Delta m)(H_{lv} + Q)] / A = \alpha E_{solar} - E_{rad} - E_{conv} - E_{cond} \quad (3)$$

$$(\Delta m)(H_{lv} + Q) = ARq_{solar} - A\varepsilon\sigma(T_1^4 - T_2^4) - Ah(T_1 - T_2) - Aq_{water} \quad (4)$$

where E_{eva}, E_{solar}, E_{rad}, E_{conv}, and E_{cond} represent the used energy for water evaporation, solar energy, thermal radiation, convection, and conduction. α is the solar absorptance of the irradiated solar light, A is an exposed/interested surface area, R is percentage of reflection, q_{solar} is solar energy (1 $kW \cdot m^{-2}$), ε is emissivity of the absorbing surface (~0.97), σ is the Stefan – Boltzmann constant (5.67×10^{-8} $W \cdot m^{-2} K^{-4}$), $T_{1,2}$ is the temperature at interested areas, h is the convection heat transfer coefficient (≈ 10 $W \cdot m^{-2} K^{-1}$), and q_{water} is the heat flow to the underlying water.

Effect of light absorption and reflection at the evaporator surface

As the absorption of the 5CS/Aga-MW reached up to 97 %, which is 3% of reflection could obtain as shown in Fig. S5b.

Effect of the heat radiation

$$A\varepsilon\sigma(T_1^4 - T_2^4) \quad (5)$$

The heat radiation was calculated with incorporation of ε is emissivity of the absorbing surface (~0.97) and σ is the Stefan – Boltzmann constant (5.67×10^{-8} $W \cdot m^{-2} K^{-4}$), presented in the equation. In the experiment, A is the surface area of evaporator at any interested area, and ΔT is the temperature different between environment and evaporator surface. The energy could be loss at the top of evaporator surface while it could be gained at the side-wall surface due to the lower temperature at the side wall relative to the environmental temperature.

Effect of the heat convection

$$Ah(T_1 - T_2) \quad (6)$$

The heat convection was calculated as shown in above equation, where h is the convection heat transfer coefficient (≈ 10 $W \cdot m^{-2} K^{-1}$). Likewise, A is the surface area of evaporator at any interested area, and ΔT is the temperature different between environment and evaporator surface. Since the temperature at the top surface of evaporator was higher than environment, so the energy could be loss to environment. On the other hand, the temperature at the side wall is lower than the environment, the additional energy from environment could receive.

Loss of the heat conduction in water

Since 10 mm of evaporator was soak into bulk water, the conductive loss could be happened. The heat loss due to the conduction could be from both the water pumping effect and the steady soaking phenomena. The equation below was calculated based on the conductive heat loss.

$$q = cm(\Delta T) \quad (7)$$

where q represents to heat flux, c is the specific heat capacity of water (4.2 kJ $°C^{-1}$ kg^{-1}), m is the bulk water used in the experiment, ΔT is the temperature of the bulk water during the time of 60 min.

Table S1. Summary of the energy flow of the 5 and 7CS/Aga-MW sponge evaporator under one sun irradiation

Evaporator	**Temperature different in bulk water (ºC)***	**E_{rad} loss (W)**	**E_{conv} loss (W)**	**E_{cond} loss (W)**
5CS/Aga-MW	9.9	0.016	0.0245	0.2888
7CS/Aga-MW	12.3	0.023	0.0343	0.3588

***** The temperature difference in bulk water before and after 1-h solar light irradiation

10. The relation between height and energy exchange between the top and side wall of the 5CS/Aga-MW

According to energy conservative rule, the energy exchange with the environment in the form of either energy loss and gain due to the 3D solar evaporator can be explained regarding to the following parameters as shown in Fig. S9b, Equation 8 and 9.[12]

$$E_t = A_t R q_{solar} - A_t \varepsilon \sigma (T_t^4 - T_{env}^4) - A_t h (T_t - T_{env}) \quad (8)$$

$$E_s = A_s \varepsilon \sigma (T_{env}^4 - T_s^4) + A_s h (T_{env} - T_t) - \kappa (T_s - T_w) \quad (9)$$

where E_t and E_s represents the energy at the top surface and side-walled surface (included with the surface area of evaporator under water), respectively, A_t is the surface area at the top surface, A_s is the surface area at the side surface, T_t is the temperature at the top surface, T_{env} is the temperature from the environment, T_s is the temperature at the side surface, T_w is the temperature at the bulk water, and κ is the thermal conductivity of vapor generator saturated with water. The thermal conductivity, κ, of evaporators is assumed to be same as that of water since the sponge evaporator continuously fills with water throughout the process.

For the height of 60 mm above water reservoir, the solar light exposed at the top surface area of the 5CS/Aga-MW was 4.9×10^{-4} m^2 (A_t), which is fixed at any height of evaporator. The side surface area of 4.7×10^{-3} m^2 (A_s) was used for energy gain from the environment calculation. The temperatures during the one sun irradiation process at equilibrium were 30, 23, 23.7, and 28 ºC for T_t, T_s, T_w, and $T_{env,}$ respectively. According to Equation 8 and 9, E_t was 1.4543 W, and the E_s was 0.3908 W. The extra energy from the side surface of 60 mm-height increased was gained and contributed to the system.

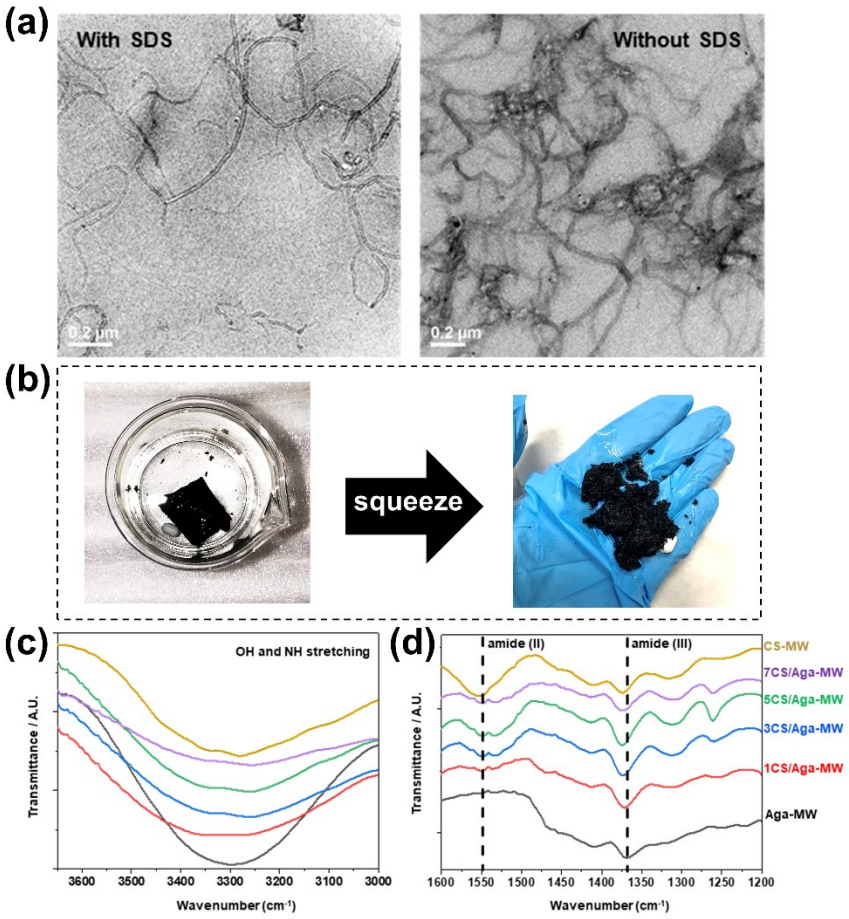

11. Figures

Fig. S1. (a) TEM images of the 5CS/Aga-MW sponge evaporator with and without SDS; (b) disintegration of Aga-MW after 24 h of stirring in water at room temperature, then squeezing; FT-IR of the bio-based composite sponge evaporators, representing the region of (c) OH-NH stretching and (d) amide II and III functional group

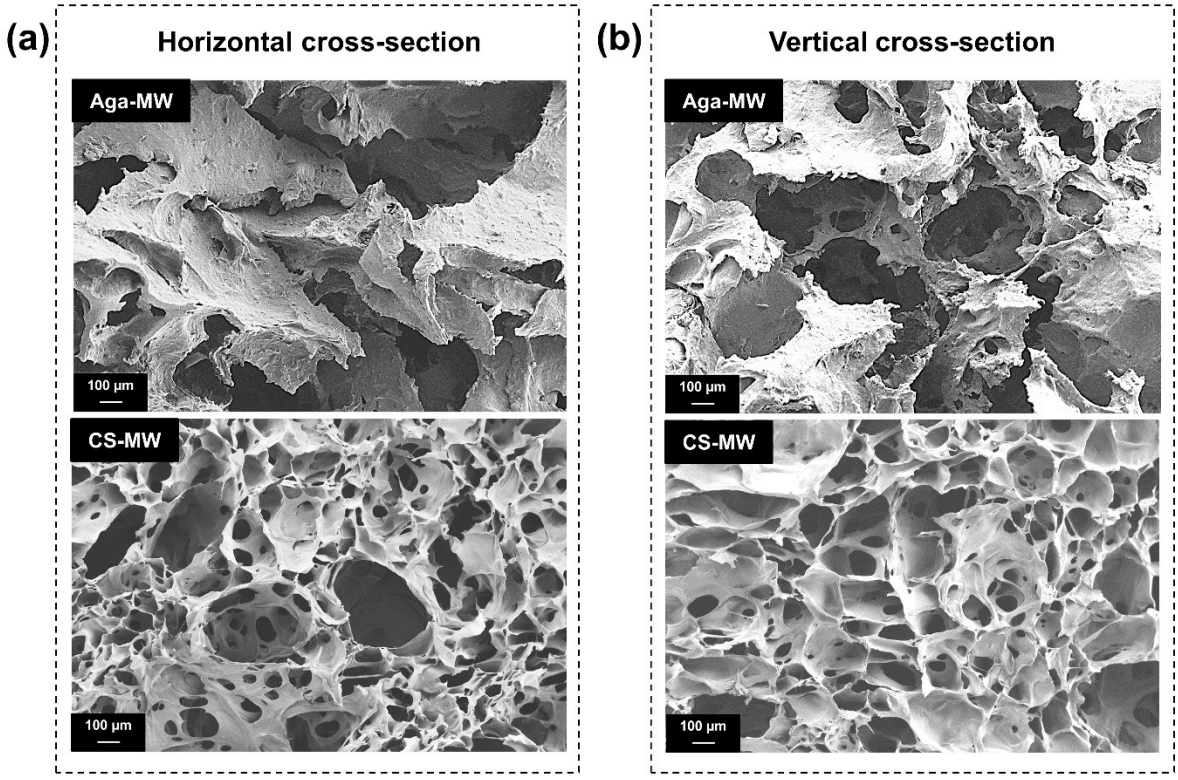

Fig. S2. SEM images of the Aga-MW and the CS-MW in (a) horizontal and (b) vertical cross-section

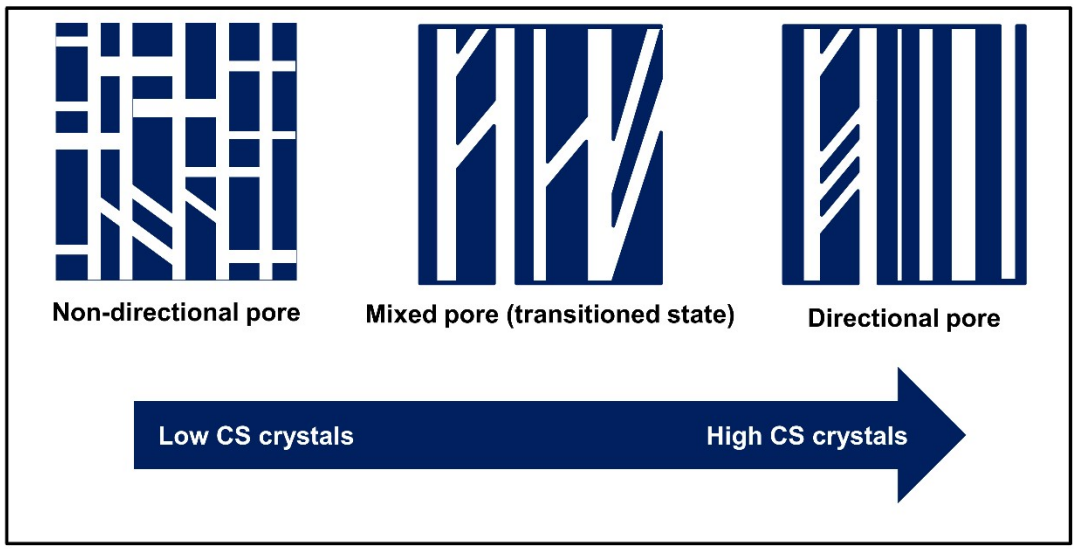

Fig. S3. schematic diagram of pore structure transformation influenced by CS crystals

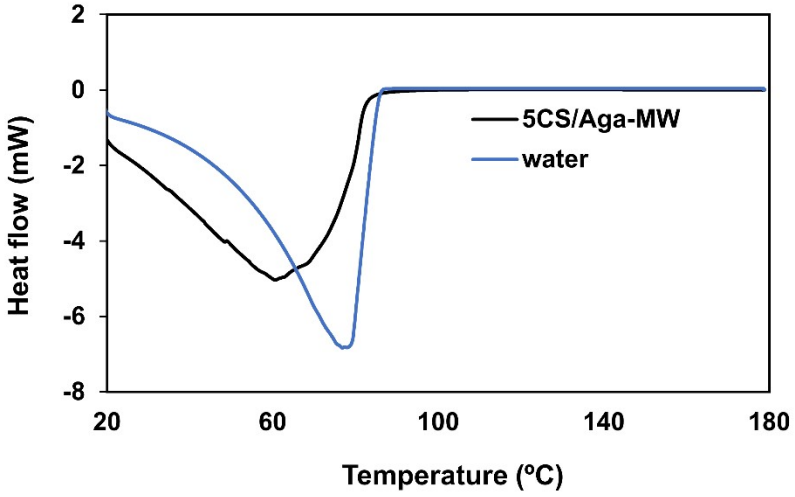

Fig. S4. DSC curve of bulk water and 5CS/Aga-MW sponge evaporator, calculating vaporization enthalpy of bulk water (2243 J/g) and water in the 5CS/Aga-MW (1995.0 J/g)

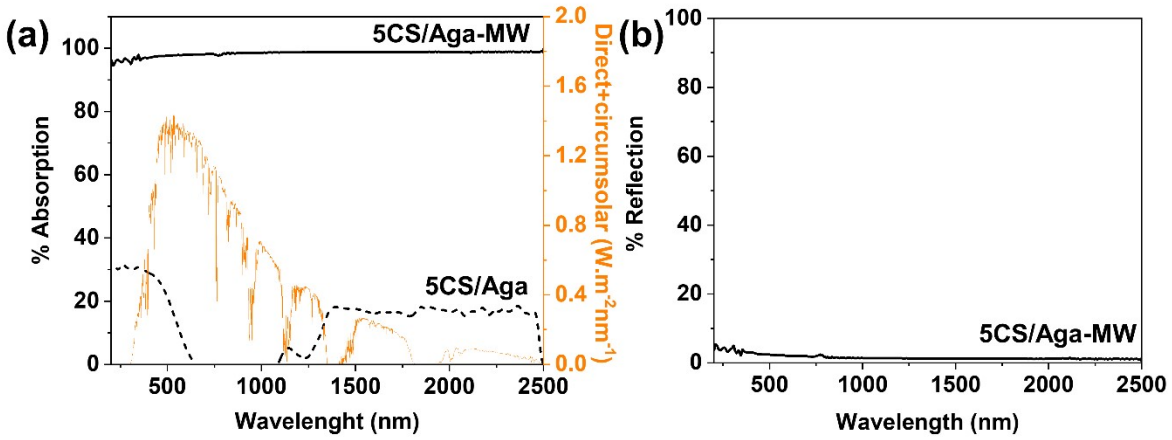

Fig. S5. (a) Absorption spectra and (b) diffuse reflection spectrum of the 5Cs/Aga with and without MW

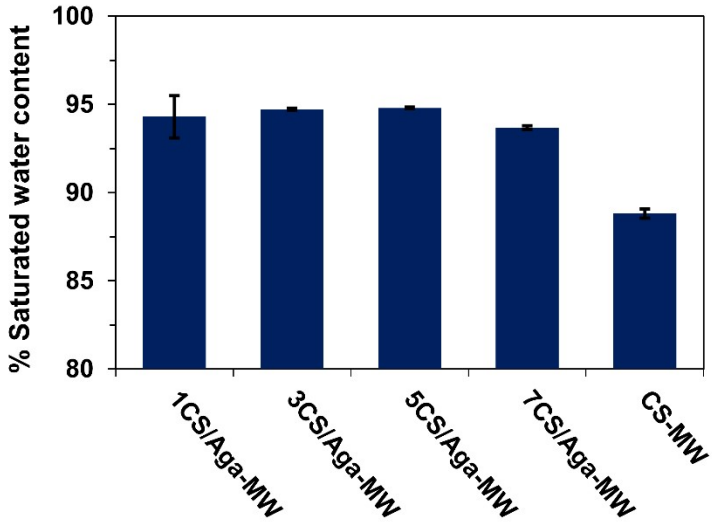

Fig. S6. Saturated water content of the 1, 3, 5, 7CS/Aga, and CS-MW

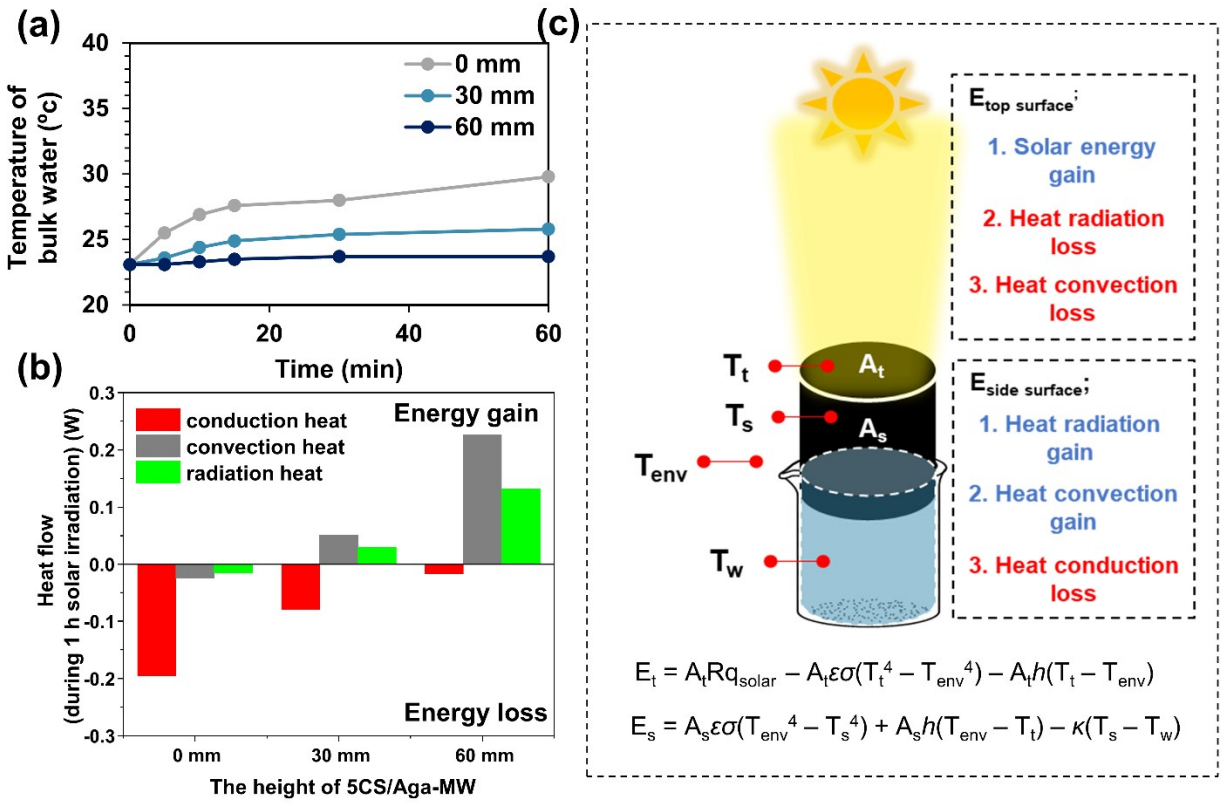

Fig. S7. (a) The temperature in the bulk water during the solar evaporation test; (b) the calculated energy loss and gain at different evaporator height and (c) schematic diagram of heat energy and temperature exchange for 3D solar evaporator related to the equations

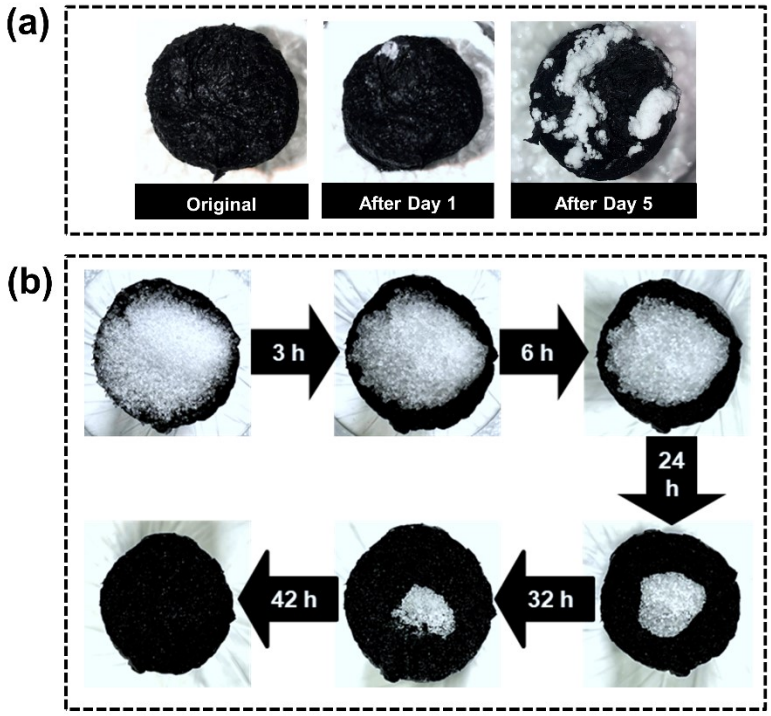

Fig. S8. (a) Digital images of the 5CS/Aga-MW at 60 mm-high before cycling experiments, after the day 1, and after the day 5 and (b) the simulated salt regeneration test of the 60 mm-height 5CS/Aga sponge evaporator

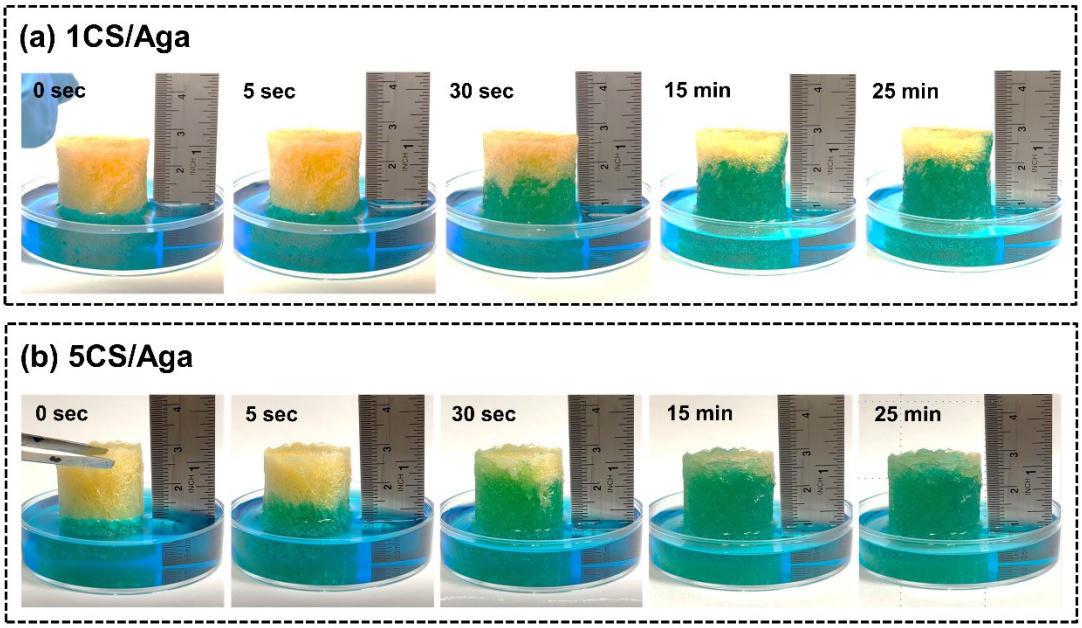

Fig. S9. Video still of water transport test of the 30 mm - (a) 1CS/Aga and (b) 5CS/Aga sponge, using methylene blue solution to vertically monitor

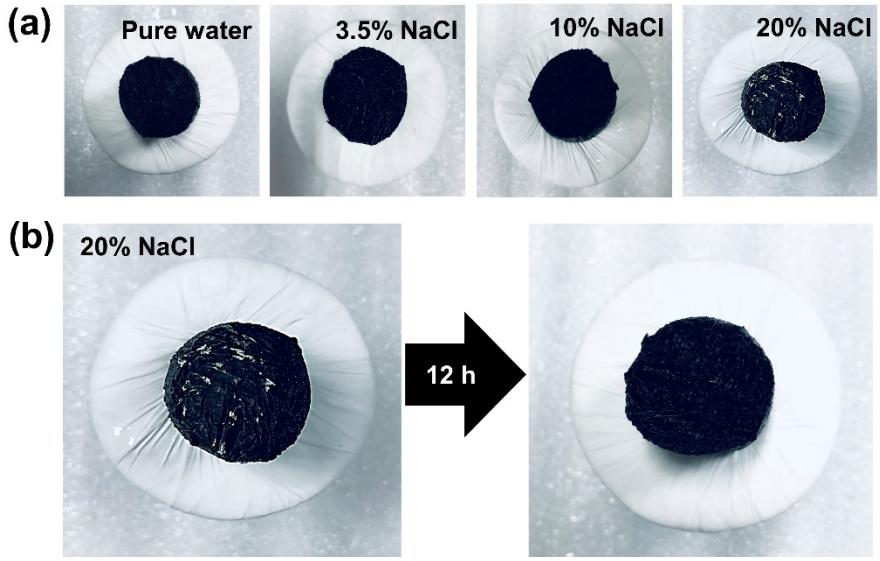

Fig. S10. (a) The salt precipitation on the surface of the 5CS/Aga-MW at different concentration of NaCl of 0% wt, 3.5% wt, 10% wt, 20% wt and (b) the self-regeneration test of the 5CS/Aga-MW in 20% wt NaCl after 12 h without solar light irradiation

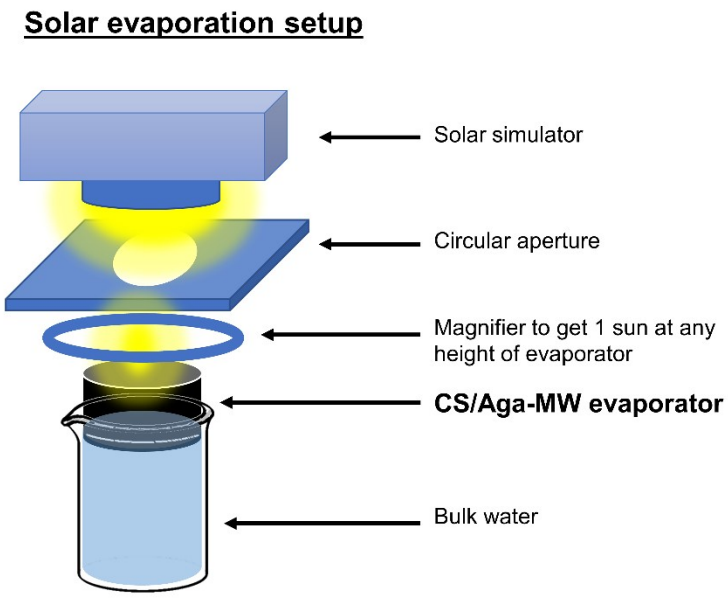

Fig. S11. The solar evaporation test setup for testing our CS/Aga-MW evaporators

Table S2. Solar evaporation performance of the 5CS/Aga-MW sponge evaporator compared with recent literature reports in the past few years

Solar evaporators	**3D Evaporator shape**	**Water evaporation rate ($kg.m^{-2}h^{-1}$)**	**Duration of one sun solar desalination without interference**	**Conc. of NaCl/seawater (%)**	**Journal**	**Ref.**
Carbonized wood	50 mm height-monolithic structure	3.91	NA	NA	ACS Appl. Mater. Interfaces 12 (2020)	13
PSS/Agarose - silver (Ag)	monolithic structure	2.10	NA	NA	Advanced Functional Materials 29 (2019)	14
PVA/nanoink - CB	10 mm height-monolithic structure	2.15	NA	NA	Nano Energy 55 (2019)	15
Cellulose/wood - CNT	60 mm height-monolithic structure	2.95	NA	NA	Nano Lett. 20 (2020)	16
Stackable nickel – cobalt/PDA	60 mm height-monolithic structure	2.42	NA	NA	J. Mater. Chem. A 8 (2020)	17
Setaria viridis - PPy	60 mm height-monolithic structure	3.72	NA	NA	ACS Appl. Mater. Interfaces 13 (2021)	18
PEDOT:PSS/PVA - MWCNT	monolithic structure	4.67	8 h continuous	3.5	Nano Energy 93 (2022)	19
Cellulose/PVA - cellulose MWCNT	12 mm height-monolithic structure	1.90	1 h / 5 days	3.5	ACS Appl. Mater. Interfaces 13 (2021)	20
SiO_2/cellulose nanofiber - CNT	monolithic structure	1.25	100 h continuous	3.5	J. Mater. Chem. A 7 (2019)	21
Carbonized chitosan	25 mm height-monolithic structure	1.76	1 h	3.5	ACS Appl. Mater. Interfaces 13 (2021)	22
Carbonized Janus wood	10 mm height-monolithic structure	1.20	8 h / 12 days	10	Energy Environ. Sci. 14 (2021)	23
Acrylic ester resin - carbon nanofiber	Arch bridge design	1.59	200 h continuous	10	Adv. Mater. 33 (2021)	24
Cotton/SA/PVA - rGO	Modified rope design	4.50	12 h / 5 days	3.5	J. Mater. Chem. A 9 (2021)	25
Chitosan - carbon powder	20 mm height-monolithic structure	1.70	6 h / 60 days	3.5	Global Challenges 5 (2021)	26

Table S2. Solar evaporation performance of the 5CS/Aga-MW sponge evaporator compared with recent literature reports in the past few years (cont.)

Solar evaporators	**3D Evaporator shape**	**Water evaporation rate ($kg.m^{-2}h^{-1}$)**	**Duration of one sun solar desalination without interference**	**Conc. of NaCl/seawater (%)**	**Journal**	**Ref.**
PVA - PDA	Aligned millineedle Arrays	2.94	13 h continuous	25	Small 17 (2021)	27
Radish-MWCNTs/PVDF - HFP layer	6 mm height-monolithic structure	2.35	8 h / 10 days	20	Desalination 510 (2021)	28
a-MoC_{1-x} - CB film	Cone structure	2.80	12 h / 30 days	3.5	Energy Environ. Sci. 14 (2021)	29
Melamine sponge - biomass CB	monolithic structure	1.54	1 h / 10 days	3.5	Environ. Sci.: Water Res. Technol. 7 (2021)	30
PVA - Mxene	Cone structure	2.20	8 h / 7 days	3.5	Adv. Funct. Mater. (2021)	31
PU - CNT	monolithic structure	1.32	2 h	25	ACS Appl. Mater. Interfaces 14 (2022)	32
Melamine sponge - thermalized $NH_4H_2PO_4$	monolithic structure sponge	2.20	24 h continuous	11	ACS Nano 16 (2022)	33
Calcined porous - TiC/C absorber	monolithic structure structure	1.75	1 h / 50 days	15	Materials Today Energy 26 (2022)	34
CS/Aga - MW	**30 mm height-monolithic structure**	**2.19**	**8 h / 10 days**	**3.5**	**This work**	-
CS/Aga - MW	**60 mm height-monolithic structure**	**3.04**	**8 h / 2 days**	**3.5**	**This work**	-

References

1. J. P. Chaudhary, S. K. Nataraj, A. Gogda and R. Meena, *Green Chemistry*, 2014, **16**, 4552-4558.
2. Q. Cao, Y. Zhang, W. Chen, X. Meng and B. Liu, *Int J Biol Macromol*, 2018, **106**, 1307-1313.
3. R. M. Felfel, M. J. Gideon-Adeniyi, K. M. Zakir Hossain, G. A. F. Roberts and D. M. Grant, *Carbohydrate Polymers*, 2019, **204**, 59-67.
4. S. Saeedi Garakani, M. Khanmohammadi, Z. Atoufi, S. K. Kamrava, M. Setayeshmehr, R. Alizadeh, F. Faghihi, Z. Bagher, S. M. Davachi and A. Abbaspourrad, *International Journal of Biological Macromolecules*, 2020, **143**, 533-545.
5. X. Li, G. Ni, T. Cooper, N. Xu, J. Li, L. Zhou, X. Hu, B. Zhu, P. Yao and J. Zhu, *Joule*, 2019, **3**, 1798-1803.
6. C. Chen, Y. Kuang and L. Hu, *Joule*, 2019, **3**, 683-718.
7. D. P. Storer, J. L. Phelps, X. Wu, G. Owens, N. I. Khan and H. Xu, *ACS Applied Materials & Interfaces*, 2020, **12**, 15279-15287.
8. B. Shao, Y. Wang, X. Wu, Y. Lu, X. Yang, G. Y. Chen, G. Owens and H. Xu, *Journal of Materials Chemistry A*, 2020, **8**, 11665-11673.
9. Z. Zhu, Y. Xu, Y. Luo, W. Wang and X. Chen, *Journal of Materials Chemistry A*, 2021, **9**, 702-726.
10. H. Li, Z. Yan, Y. Li and W. Hong, *Water Research*, 2020, **177**, 115770.
11. W. Zhang, G. Zhang, Q. Ji, H. Liu, R. Liu and J. Qu, *ACS Applied Materials & Interfaces*, 2019, **11**, 9974-9983.
12. X. Li, J. Li, J. Lu, N. Xu, C. Chen, X. Min, B. Zhu, H. Li, L. Zhou, S. Zhu, T. Zhang and J. Zhu, *Joule*, 2018, **2**, 1331-1338.
13. J. Tang, T. Zheng, Z. Song, Y. Shao, N. Li, K. Jia, Y. Tian, Q. Song, H. Liu and G. Xue, *ACS Applied Materials & Interfaces*, 2020, **12**, 18504-18511.
14. Z. Sun, J. Wang, Q. Wu, Z. Wang, Z. Wang, J. Sun and C.-J. Liu, *Advanced Functional Materials*, 2019, **29**, 1901312.
15. Z. Deng, L. Miao, P.-F. Liu, J. Zhou, P. Wang, Y. Gu, X. Wang, H. Cai, L. Sun and S. Tanemura, *Nano Energy*, 2019, **55**, 368-376.
16. Q.-F. Guan, Z.-M. Han, Z.-C. Ling, H.-B. Yang and S.-H. Yu, *Nano Letters*, 2020, **20**, 5699-5704.
17. B. Shao, Y. Wang, X. Wu, Y. Lu, X. Yang, G. Y. Chen, G. Owens and H. Xu, *Journal of Materials Chemistry A*, 2020, **8**, 11665-11673.
18. Z. Xie, J. Zhu and L. Zhang, *ACS Applied Materials & Interfaces*, 2021, **13**, 9027-9035.
19. Y. Xu, J. Xu, J. Zhang, X. Li, B. Fu, C. Song, W. Shang, P. Tao and T. Deng, *Nano Energy*, 2022, **93**, 106882.
20. K. Liu, W. Zhang, H. Cheng, L. Luo, B. Wang, Z. Mao, X. Sui and X. Feng, *ACS Applied Materials & Interfaces*, 2021, **13**, 10612-10622.
21. R. Hu, J. Zhang, Y. Kuang, K. Wang, X. Cai, Z. Fang, W. Huang, G. Chen and Z. Wang, *Journal of Materials Chemistry A*, 2019, **7**, 15333-15340.
22. Z. Liu, R.-K. Qing, A.-Q. Xie, H. Liu, L. Zhu and S. Chen, *ACS Applied Materials & Interfaces*, 2021, **13**, 18829-18837.
23. X. Chen, S. He, M. M. Falinski, Y. Wang, T. Li, S. Zheng, D. Sun, J. Dai, Y. Bian, X. Zhu, J. Jiang, L. Hu and Z. J. Ren, *Energy & Environmental Science*, 2021, **14**, 5347-5357.
24. M. Zou, Y. Zhang, Z. Cai, C. Li, Z. Sun, C. Yu, Z. Dong, L. Wu and Y. Song, *Advanced Materials*, 2021, **33**, 2102443.
25. Y. Peng, X. Zhao and C. Liu, *Journal of Materials Chemistry A*, 2021, **9**, 22472-22480.
26. Y. Gu, X. Mu, P. Wang, X. Wang, Y. Tian, A. Wei, J. Zhang, Y. Chen, Z. Sun, J. Zhou and L. Miao, *Global Challenges*, 2021, **5**, 2000063.
27. Z. Huang, J. Wei, Y. Wan, P. Li, J. Yu, J. Dong, S. Wang, S. Li and C.-S. Lee, *Small*, 2021, **17**, 2101487.
28. B. Lv, C. Gao, Y. Xu, X. Fan, J. Xiao, Y. Liu and C. Song, *Desalination*, 2021, **510**, 115093.
29. L. Zhu, L. Sun, H. Zhang, H. Aslan, Y. Sun, Y. Huang, F. Rosei and M. Yu, *Energy & Environmental Science*, 2021, **14**, 2451-2459.

30. K. Xu, C. Wang, Z. Li, X. Yan, X. Mu, M. Ma and P. Zhang, *Environmental Science: Water Research & Technology*, 2021, **7**, 879-885.
31. L. Li, N. He, B. Jiang, K. Yu, Q. Zhang, H. Zhang, D. Tang and Y. Song, *Advanced Functional Materials*, 2021, **31**, 2104380.
32. S. Li, F. Qiu, Y. Xia, D. Chen and X. Jiao, *ACS Applied Materials & Interfaces*, 2022, **14**, 19409-19418.
33. H.-Y. Zhao, J. Huang, J. Zhou, L.-F. Chen, C. Wang, Y. Bai, J. Zhou, Y. Deng, W.-X. Dong, Y.-S. Li and S.-H. Yu, *ACS Nano*, 2022, **16**, 3554-3562.
34. M. Ma, X. Cao, K. Xu, X. Mu, X. Yan, P. Zhang and C. Wang, *Materials Today Energy*, 2022, **26**, 101009.